



The C-terminal cysteine-rich motif of NYE1/SGR1 is indispensable for its function in chlorophyll degradation in Arabidopsis

Xie, Zuokun ; Wu, Shengdong ; Chen, Junyi ; Zhu, Xiaoyu ; Zhou, Xin ; Hörtensteiner, Stefan ; Ren, Guodong ; Kuai, Benke

Abstract: KEY MESSAGE The C-terminal cysteine-rich motif of NYE1/SGR1 affects chlorophyll degradation likely by mediating its self-interaction and conformational change, and somehow altering its Mg-dechelating activity in response to the changing redox potential. During green organ senescence in plants, the most prominent phenomenon is the degreening caused by net chlorophyll (Chl) loss. NON-YELLOWING1/STAY-GREEN1 (NYE1/SGR1) was recently reported to be able to dechelates magnesium (Mg) from Chl a to initiate its degradation, but little is known about the domain/motif basis of its functionality. In this study, we carried out a protein truncation assay and identified a conserved cysteine-rich motif (CRM, P-X3-C-X3-C-X-C2-F-P-X5-P) at its C terminus, which is essential for its function. Genetic analysis showed that all four cysteines in the CRM were irreplaceable, and enzymatic assays demonstrated that the mutation of each of the four cysteines affected its Mg-dechelating activity. The CRM plays a critical role in the conformational change and self-interaction of NYE1 via the formation of inter- and intra-molecular disulfide bonds. Our results may provide insight into how NYE1 responds to rapid redox changes during leaf senescence and in response to various environmental stresses.

DOI: <https://doi.org/10.1007/s11103-019-00902-1>

Posted at the Zurich Open Repository and Archive, University of Zurich

ZORA URL: <https://doi.org/10.5167/uzh-183047>

Journal Article

Accepted Version

Originally published at:

Xie, Zuokun; Wu, Shengdong; Chen, Junyi; Zhu, Xiaoyu; Zhou, Xin; Hörtensteiner, Stefan; Ren, Guodong; Kuai, Benke (2019). The C-terminal cysteine-rich motif of NYE1/SGR1 is indispensable for its function in chlorophyll degradation in Arabidopsis. *Plant molecular biology*, 101(3):257-268.

DOI: <https://doi.org/10.1007/s11103-019-00902-1>

1 Running title: The cysteine-rich motif of NYE1 mediates its function

2 Corresponding Authors: Guodong Ren and Benke Kuai

3 ^aState Key Laboratory of Genetic Engineering and Ministry of Education Key Laboratory for
4 Biodiversity Science and Ecological Engineering, School of Life Sciences, Fudan University,
5 Shanghai 200438, China

6 ^bMinistry of Education Key Laboratory for Biodiversity Science and Ecological Engineering,
7 Institute of Biodiversity Science, Fudan University, Shanghai 200438, China

8 Tel: 86-021-31246639

9 E-mail: gdren@fudan.edu.cn; bkkuai@fudan.edu.cn

10

The C-terminal cysteine-rich motif of NYE1/SGR1 is indispensable for its function in chlorophyll degradation in *Arabidopsis*

Zuokun Xie^{1, 2}, Shengdong Wu^{1, 2}, Junyi Chen^{1, 2}, Xiaoyu Zhu^{1, 2}, Xin Zhou^{1, 2}, Stefan Hörtensteiner³, Guodong Ren^{1, 2*} and Benke Kuai^{1, 2*}

¹State Key Laboratory of Genetic Engineering and Ministry of Education Key Laboratory for Biodiversity Science and Ecological Engineering, School of Life Sciences, Fudan University, Shanghai 200438, China

²Ministry of Education Key Laboratory for Biodiversity Science and Ecological Engineering, Institute of Biodiversity Science, Fudan University, Shanghai 200438, China

³Institute of Plant and Microbial Biology, University of Zurich, Zollikerstrasse 107, CH-8008 Zurich, Switzerland

*Corresponding authors: Guodong Ren: gdren@fudan.edu.cn

Benke Kuai: bkkuai@fudan.edu.cn

Keywords: Arabidopsis, chlorophyll degradation, NYE1/SGR1, cysteine-rich motif, redox regulation

Footnotes:

Author Contributions: Conceived and designed the experiments: BK, GR, SH, ZX, JC. Performed the experiments: ZX, SW, JC, XZhu. Analyzed the data: ZX, JC. Contributed reagents/ materials/ analysis tools: XZho, SH. Wrote the paper: BK, GR, ZX, JC, SH, XZhu.

Funding information: This work was supported by grants from the National Natural Science Foundation of China (31670287) to BK, the Science and Technology Commission of Shanghai Municipality (2015JC1400800) to GR, and the Swiss National Science Foundation (31003A_172977) to SH.

Corresponding author email: gdren@fudan.edu.cn; bkkuai@fudan.edu.cn

Abstract

Key message The C-terminal cysteine-rich motif of NYE1/SGR1 affects chlorophyll degradation likely by mediating its self-interaction and conformational change, and somehow altering its Mg-dechelating activity in response to the changing redox potential.

Abstract During green organ senescence in plants, the most prominent phenomenon is the degreening caused by net chlorophyll (Chl) loss. NON-YELLOWING1/ STAY-GREEN1 (NYE1/SGR1) was recently reported to be able to dechelates magnesium (Mg) from Chl *a* to initiate its degradation, but little is known about the domain/motif basis of its functionality. In this study, we carried out a protein truncation assay and identified a conserved cysteine-rich motif (CRM, P-X3-C-X3-C-X-C2-F-P-X5-P) at its C terminus, which is essential for its function. Genetic analysis showed that all four cysteines in the CRM were irreplaceable, and enzymatic assays demonstrated that the mutation of each of the four cysteines affected its Mg-dechelating activity. The CRM plays a critical role in the conformational change and self-interaction of NYE1 via the formation of both intra- and inter-molecular disulfide bonds. Our results may provide insight into how NYE1 responds to rapid redox changes during leaf senescence and in response to various environmental stresses.

INTRODUCTION

Degreening caused by rapid chlorophyll (Chl) degradation is a process integral to green organ senescence in plants. It is not only a prerequisite for the degradation of Chl-binding proteins and consequently remobilization of a significant proportion of nutrients in senescing organs (Christ et al., 2014), but also vital for the detoxification of potentially photoactive Chls (Li et al., 2017). Recently, the biochemical pathway of Chl degradation, termed as the PAO/phyllobilin pathway, was elucidated (Christ et al., 2014, Kuai et al., 2018). Before entering the degradation pathway, Chl *b* is converted to Chl *a* through a two-step reaction (Sato et al., 2009, Meguro et al., 2011). Chl *a* is degraded via three major steps, magnesium de-chelation (Shimoda et al., 2016, Matsuda et al., 2016), dephytylation (Ren et al., 2010, Schelbert et al., 2009), and porphyrin macrocycle opening, to generate a linear red Chl catabolite (RCC) (Gray et al., 1997, Pruzinska et al., 2003), which is consecutively reduced to a primary fluorescent Chl catabolite (*p*FCC) (Pruzinska et al., 2007). *p*FCC is then modified to the end products, named phyllobilins (Krautler, 2014), by a series of enzymes, and finally stored in vacuoles (Christ et al., 2012, Christ et al., 2013, Hauenstein et al., 2016).

NON-YELLOWING1/STAY-GREEN1 (NYE1/SGR1; named NYE1 in the following) was initially identified as a key regulator of Chl degradation in multiple species (Armstead et al., 2006, Jiang et al., 2007, Park et al., 2007, Ren et al., 2007, Sato et al., 2007, Aubry et al., 2008, Barry et al., 2008, Borovsky and Paran, 2008, Mecey et al., 2011, Zhou et al., 2011, Fang et al., 2014). In particular, it was shown to be responsible for Mendel's green cotyledon trait (Sato et al., 2007, Armstead et al., 2007). Based on its extensive interactions with Chl catabolic enzymes (CCEs) and the subunits of light-harvesting complex II (LHCII), it was once postulated that it might act to recruit CCEs to somehow facilitate an efficient degradation of Chls (Sakuraba et al., 2012). However, this has not been further verified. By contrast, Shimoda et.al (2016) demonstrated that NYE1 expressed in the wheat germ system has an activity of dechelating Mg^{2+} from Chl *a*, solving a long-lasting mystery as for whether the first step of Chl *a* degradation is an enzymatic process and if yes, which enzyme(s) is responsible for it (Shimoda et al., 2016, Matsuda et al., 2016). Interestingly, NYE1 and its orthologs have also been implicated in other biological processes, e.g. disease resistance and symptom developments in *Arabidopsis thaliana* (Arabidopsis) and cucumber (Mur et al., 2010, Mecey et al., 2011, Pan et al., 2018), nodule senescence in *Medicago truncatula* (Zhou et al., 2011), lycopene and β -carotene synthesis during tomato ripening (Luo et al., 2013), and oil accumulation in *Brassica napus* (Qian et al., 2016).

Over the past few years, the transcriptional regulation of *NYE1* during degreening and senescence has been extensively exploited. Our previous work showed that MYC2/3/4, EIN3,

ORE1, ABF2/3/4, PIF4, and ANAC019/055/072 transcription factors (TFs) positively regulate the expression of *NYE1* and/or its paralog *NYE2* during *Arabidopsis* leaf senescence in a hormone- and dark condition-dependent manner, whereas SOC1 negatively regulates the expression of *NYE1* (Song et al., 2014, Qiu et al., 2015, Zhu et al., 2015, Gao et al., 2016, Li et al., 2016, Zhu et al., 2017, Kuai et al., 2018, Chen et al., 2017). It has also been reported that ABI3 positively regulates the expression of both *NYE1* and *NYE2*, promoting the degradation of Chl during seed maturation (Delmas et al., 2013), and ABI5 and EEL, both of which function downstream of PIF4/5, promote the expression of *NYE1* (Sakuraba et al., 2014a).

NYE1 protein orthologs of many higher plants, as well as respective paralogs that are found in many species, are highly conserved. They exhibit two major domains, i.e. a large core domain and a C-terminal domain, which are separated by a rather variable region (Hörtensteiner, 2009). Several reported point mutations located in the conserved core domains cause a significant defect in Chl degradation, suggesting a functional importance of respective conserved residues (Park et al., 2007, Jiang et al., 2007, Barry et al., 2008, Borovsky and Paran, 2008, Mecey et al., 2011). Until now, however, no biochemical functions for the conserved C-terminal domain have been unveiled. In this study, by a protein truncation assay, we identified that the C-terminal domain, i.e. *NYE1*²¹²⁻²⁴², containing a cysteine-rich motif (CRM), is required for its function in Chl degradation. Further analyses showed that the CRM is necessary for the Mg-dechelation activity of *NYE1*. In addition, the CRM facilitates the conformational change of *NYE1* via the formation of both intra- and inter-molecular disulfide bonds.

RESULTS

The C-terminal CRM of *NYE1* is crucial for its function

To investigate the molecular basis of *NYE1*'s function, we performed a protein truncation assay to identify its key functional domains and/or motifs. A series of truncated fragments were generated according to the conservation pattern of *NYE1* protein sequences among higher plants (Figure 1a, Figure S1). The cDNAs of these fragments were individually inserted into the pCHF3 vector driven by the CaMV 35S promoter, and the resulting constructs were transiently expressed in *N. benthamiana* leaves. Two days post infiltration, leaves of *N. benthamiana* expressing the full-length *NYE1* (*NYE1*¹⁻²⁶⁸) or *NYE1*¹⁻²⁴² exhibited yellowish phenotypes. By contrast, those expressing *NYE1*¹⁻²¹¹ or other shorter fragments stayed green (Figure 1b), suggesting that deletion of the *NYE1*²¹²⁻²⁴² fragment leads to malfunction of *NYE1*. Our previous studies showed that overexpression of *NYE1* caused a yellowing leaf phenotype, particularly in the younger leaves of *Arabidopsis* plants (Ren et al.,

2007, Wu et al., 2016). To verify this result, the constructs containing the truncated *NYE1* fragments were introduced into the *nye1-1* mutant background. After obtaining T1 transgenic plants, we found that a majority of the plants expressing the full-length *NYE1* (*NYE1*¹⁻²⁶⁸) or *NYE1*¹⁻²⁴² exhibited albino or yellowish leaves, which is consistent to our previous reports. By contrast, all plants expressing *NYE1*¹⁻²¹¹ or other shorter fragments showed no obvious phenotypic changes (Figure 1c), indicating unsuccessful complementation of *nye1-1*. To further validate the observations, we introduced the cDNA fragments of both *NYE1*¹⁻²¹¹ and *NYE1*¹⁻²⁴² driven by a 1.5 kb promoter fragment of *NYE1* into *nye1-1* and treated excised 5-6th true leaves from both *P_{NYE1}::NYE1*¹⁻²¹¹ and *P_{NYE1}::NYE1*¹⁻²⁴² transgenic plants in darkness for five days. As expected, *P_{NYE1}::NYE1*¹⁻²⁴², but not *P_{NYE1}::NYE1*¹⁻²¹¹, rescued the stay-green phenotype of *nye1-1* (Figure 1d). These results collectively suggest that the *NYE1*²¹²⁻²⁴² fragment is essential for the function of *NYE1* in Chl degradation.

A multiple protein sequence alignment showed that the *NYE1*²¹²⁻²⁴² region contains a CRM, as previously described (Aubry et al., 2008), that includes eight invariable amino acids (P-X3-C-X3-C-X-C2-F-P-X5-P) (Figure 2a). To investigate whether four cysteines in the CRM are necessary for *NYE1*'s function, we mutated all the four cysteines to both alanine (*NYE1*^{C224A/C228A/C230A/C231A}, named as *NYE1*^{4C→4A}) and glycine (*NYE1*^{C224G/C228G/C230G/C231G}, named as *mNYE1*), because we noticed that cysteine residues were mutated interchangeably either to glycine or to alanine residues by different labs. We further constructed *35S::NYE1*^{4C→4A}-*FLAG* and *35S::mNYE1*-*FLAG* vector and examined their function in *N. benthamiana* leaves. As shown in Figure S2, the phenotypes of *N. benthamiana* leaves expressing *NYE1*^{C224A/C228A/C230A/C231A}-*FLAG* were similar to the ones of those expressing *NYE1*^{C224G/C228G/C230G/C231G}-*FLAG*. To investigate whether other conserved residues in CRM are responsible for *NYE1* functionality, we carried out an alanine (Ala) scanning mutagenesis assay. The eight conserved residues were individually mutated to Ala, and the mutated cDNAs introduced into the *nye1-1* background. While a majority of T1 transgenic plants expressing *NYE1*^{P220A}, *NYE1*^{F232A}, *NYE1*^{P233A}, or *NYE1*^{P239A} exhibited albino or yellowish leaves, only few transgenic plants expressing *NYE1*^{C224A}, *NYE1*^{C228A}, *NYE1*^{C230A} or *NYE1*^{C231A} showed yellowing leaf phenotypes (Figure 2b), suggesting that all the four cysteines in the CRM significantly affect *NYE1* function.

There are additional four cysteines (C2, C135, C156 and C201) scattering upstream of the CRM, among which C135 and C201 are highly conserved (Figure S1). To evaluate the contribution of these cysteines to *NYE1* function, we generated single cysteine to alanine mutations and performed transient expression assays in the leaves of *N. benthamiana*. Leaves expressing *NYE1*^{C2A}, *NYE1*^{C135A}, *NYE1*^{C156A}, and *NYE1*^{C201A} triggered chlorophyll

degradation as the wild-type NYE1 did (Figure 2c), suggesting that these cysteine residues were not as critical as the four ones residing within the CRM.

Thus far, five point mutations of NYE1 have been reported to cause a functional defect in Chl degradation in different plant species (Park et al., 2007, Jiang et al., 2007, Barry et al., 2008, Borovsky and Paran, 2008, Mecey et al., 2011). We produced corresponding mutations in *Arabidopsis* NYE1, and infiltrated the resulting expression constructs (NYE1^{Y82C}-FLAG, NYE1^{D88Y}-FLAG, NYE1^{I97M}-FLAG, NYE1^{W122R}-FLAG and NYE1^{R151S}-FLAG) into *N. benthamiana* leaves. Consistently, no obvious yellowing symptoms were observed with these mutant constructs, in contrast to the yellowing symptoms developed after infiltration with the wild-type NYE1 construct (Figure 2d).

The CRM guarantees the Mg-dechelating activity of NYE1

NYE1, as well as NYE2, catalyzes the removal of Mg²⁺ from Chl *a* to generate pheophytin *a* (phein *a*), which is subsequently dephytylated by PPH (Schelbert et al., 2009, Shimoda et al., 2016). We reasoned that blocking of the Mg-dechelation step would abolish the generation of phein *a*, which is over-accumulated during leaf senescence when the function of PPH is compromised (Schelbert et al., 2009). To test this, we generated the *nye1 nye2 ppH* triple mutant by crossing. The triple mutant showed a strong stay-green phenotype resembling that of the *nye1 nye2* double mutant after 4 d of dark incubation (Figure 3a). Remarkably, phein *a* was not detectable in the triple mutant (Figure 3b), genetically confirming that both NYE1 and NYE2 function upstream of PPH.

To investigate whether the CRM motif affects the Mg-dechelating activity of NYE1, we analyzed the Mg-dechelating activity of recombinant NYE1-FLAG and mNYE1-FLAG (NYE1^{C224G/C228G/C230G/C231G}), in which all the four cysteines in the CRM were mutated to glycine, prepared by using the wheat germ protein expression system (Shimoda et al., 2016) (Figure 3c). Recombinant NYE1-FLAG showed a robust, albeit low Mg-dechelating activity, whereas mNYE1-FLAG exhibited no Mg-dechelating activity at all when Chl *a* was used as the substrate (Figure 3d). This result suggests that the CRM is necessary for the Mg-dechelating activity of NYE1.

To further investigate whether other conserved residues affects the Mg-dechelating activity of NYE1, we examined the enzymatic activity of five reported point mutants of NYE1 as described above (Figure 2d). It was shown that all the five residues were essential for the Mg-dechelating activity of NYE1 (Figure S3a-b), including the D88Y substitution, which affects the development of disease symptoms (Mecey et al., 2011).

The CRM facilitates the self-interaction of NYE1

NYE1 and NYE2 form homo- and/or heterodimers during leaf senescence (Sakuraba et al., 2014c). To clarify whether the CRM affects NYE1 self-interaction, we performed *in vitro* pull-down assays. MBP, MBP-NYE1, or MBP-mNYE1 were individually mixed with His-NYE1 and incubated with amylose resin. The pulled-down fractions were subjected to SDS-PAGE and analyzed by immunoblotting using a monoclonal anti-His antibody. The results showed that MBP-NYE1 pulled down more His-NYE1 proteins than MBP-mNYE1 (Figure 4a). Similar results were obtained from the reverse pull-down assay using Ni-NTA resin (Figure 4b). Furthermore, we carried out bimolecular fluorescence complementation (BiFC) assays to verify the above results. Full-length NYE1 and mNYE1 were fused to either the N- or C-terminal half of yellow fluorescent protein (YFP), and co-expressed in tobacco leaves. A stronger YFP fluorescence signal was generated with the combination of NYE1-nYFP and NYE1-cYFP rather than with that of mNYE1-nYFP and NYE1-cYFP (Figure 4c). To investigate whether NYE1 self-interaction is dependent on the disulfide bonds, we examined the self-interaction ability of NYE1 under both non-reducing and reducing condition using a MBP pulldown assay. As shown in Figure S4, 5mM DTT reduced but not complete blocked NYE1 self-interaction, suggesting that both disulfide bonds and other unknown bonds affect the NYE1 self-interaction. Taken together, these results suggest that the four cysteines in the CRM facilitate NYE1 self-interaction.

NYE1 interacts with other CCEs during leaf senescence (Sakuraba et al., 2012). To investigate whether the CRM affects the interaction between NYE1 and other CCEs, we performed further *in vitro* pull-down assays. His-NYE1, His-mNYE1, and MBP-CCEs were expressed in *E. coli*, mixed and incubated with Ni-NTA resin, respectively. Western blot analysis revealed that the amounts of pulled-down MBP-CCEs were similar with His-NYE1 or His-mNYE1 (Figure S5a). Consistent results were observed in BiFC assays, i.e. the intensity of YFP fluorescence generated with the combinations of NYE1-nYFP and CCEs-cYFP was visually similar to that with the combinations of mNYE1-cYFP and CCEs-cYFP (Figure S5b), suggesting that the CRM is not required for NYE1 to interact with other CCEs during leaf senescence.

NYE1 also interacts with LHCII complex during leaf senescence (Park et al., 2007, Sakuraba et al., 2012). To investigate whether the CRM affects the interaction between NYE1 and LHCII complex, the cDNAs of NYE1 truncated versions were constructed to pGADT7 (AD) vectors, and those of Lhcb1, Lhcb2 and Lhcb3 constructed to pGBKT7 (BD) vectors. The interaction capabilities of different NYE1 truncated versions with Lhcb subunits were

examined by the yeast-two-hybrid assay. As shown in Figure S5c, NYE1⁴⁹⁻²⁶⁸ (Full length with chloroplast transit peptide removed) and NYE1⁴⁹⁻⁷¹ interacted with all three Lhcb proteins, and NYE1¹³¹⁻²¹¹ interacted with Lhcb2 and Lhcb3 but not Lhcb1. In contrast, the NYE1²¹²⁻²⁶⁸, which contains the CRM motif, did not interact with all three Lhcbs, suggesting that CRM is not required for NYE1 to interact with LHCII complex during leaf senescence.

The CRM domain is involved in the redox regulation of NYE1 conformations

Cysteine residues are often involved in disulfide bridge formation to regulate conformation and/or activity changes (Giles et al., 2003). To clarify whether the CRM is involved in the formation of disulfide bonds, NYE1-FLAG and mNYE1-FLAG fusion proteins were transiently expressed in the leaves of *N. benthamiana*. Time-course experiments showed that leaves expressing NYE1-FLAG began to turn yellow 24 h after infiltration and the yellowing phenotype became more severe at the later time points. However, little change was observed in the leaves expressing mNYE1-FLAG or empty vector (Figure 5a). Immunoblot analysis revealed that both NYE1-FLAG and mNYE1-FLAG existed as monomeric forms 24 h after infiltration, and gradually formed dimers and oligomers at 36 h and 48 h under non-reducing conditions (Figure 5b). We noticed that the monomeric form of NYE1-FLAG migrated faster than mNYE1-FLAG in the gel, implying that the CRM may be involved in the formation of intramolecular disulfide bond. In addition, the proportion of oligomerized NYE1-FLAG was higher than that of oligomerized mNYE1-FLAG, suggesting that the CRM may affect the oligomerization of NYE1. After treatment with 5 mM DTT, the electrophoretic mobility of monomeric NYE1-FLAG became similar to that of mNYE1-FLAG (Figure 5c), confirming that the CRM is involved in the formation of intramolecular disulfide bond. Notably, the dimers and oligomers of NYE1-FLAG and mNYE1-FLAG were depolymerized to reduced monomers, indicating that NYE1-FLAG can be oligomerized through the formation of intermolecular disulfide bonds. Free cysteine residues could form non-specific disulfide bonds during sample preparation (Mou et al., 2003). To examine whether the different conformations of NYE1 exist indeed *in vivo*, we added an alkylating agent NEM to SDS sample buffer before preparation, which could inhibit the formation of non-specific disulfide bonds. Western blot assays showed that in the presence of 5 mM NEM, NYE1-FLAG were detected primarily as reduced monomeric forms at the time-point of 24 h after infiltration (Figure 5d), implying that the oxidized monomers observed in Figure 5b were an artifact, likely being produced during sample preparation. However, oxidized dimers and oligomers were indeed detected at the time-points of 36 h and 48 h, suggesting that the dimerization and oligomerization of NYE1-FLAG do occur through oxidation during induced senescence in the cells of *N. benthamiana*. Taken together, our results indicate that the four cysteines in the CRM are involved in the formation of both intra- and inter-molecular disulfide bonds.

DISCUSSION

A cysteine-rich motif at the C terminal of NYE1 and five conserved residues in its core domain are required for its Mg-dechelating activity

NYE1 was originally identified as a key regulator of Chl degradation, and its mutation led to a stay-green phenotype during leaf senescence in *Arabidopsis* (Ren et al., 2007). NYE1 orthologous proteins are highly conserved in higher plant species (Ren et al., 2007, Hortensteiner, 2009). However, bioinformatics analysis has not provided clues about the possible functions of its conserved domains, nor have experimental data been provided. In this study, by a protein truncation assay, we identified a domain, NYE1²¹²⁻²⁴², localized at the C-terminus of NYE1, which is indispensable for its function (Figure 1). In addition, point mutagenesis assays demonstrated that all four cysteines residing in a cysteine-rich motif (CRM, P-X3-C-X3-C-X-C2-F-P-X5-P) within the NYE1²¹²⁻²⁴² region are required for NYE1 function (Figure 2b and Figure S2). By contrast, other cysteines (C2, C135, C156 and C201) localized either in the N-terminal putative chloroplast transit peptide or in the highly conserved core domain were of no functional importance (Figure 2c). Our analyses highlight the importance of the CRM for NYE1 functionality *in vivo*.

Recently, NYE1 was reported as an Mg-dechelate in the Chl degradation pathway (Shimoda et al., 2016). Consistently, we found that pheophorbide *a* did not accumulate in senescing leaves of the *nye1 nye2 pph* triple mutant (Figure 3a-b). Notably, mutations of cysteines in the CRM (mNYE1-FLAG) abolished the Mg-dechelating activity of NYE1 *in vitro* (Figure 3c-d), indicating that the CRM is necessary for NYE1 to function as an Mg-dechelate. Consistently, other five reported point mutations of NYE1 (Park et al., 2007, Jiang et al., 2007, Barry et al., 2008, Borovsky and Paran, 2008, Mecey et al., 2011) also affect the Mg-dechelating activity of NYE1 *in vitro* (Figure S3a-b). These results imply that both the core domain and the CRM are required for the Mg-dechelating activity of NYE1.

NYE1 conformation is likely regulated by redox in senescent leaf cells

Thiol groups of cysteines are often involved in the redox regulation of protein conformational changes and activity (Giles et al., 2003), e.g. C82 and C216 of NPR1 (Non-expressor of Pathogenesis Related genes 1) in *Arabidopsis* affect both its protein conformation and activity via the formation of intermolecular disulfide bonds (Mou et al., 2003). In this study, we demonstrate that NYE1 displays different conformational states during Chl degradation, including monomers, dimers, and oligomers. In addition, both monomers and dimers exhibit oxidized and reduced redox states. Mutations of the four cysteines in the CRM affected not only the oligomerization but also the redox status of NYE1 (Figure 5b-d). Thus, the CRM

may participate in the formation of both inter- and intra-molecular disulfide bonds, which is consistent with our further finding that the CRM affects NYE1 self-interaction but not its interaction with other CCEs and LHCII complex (Figure 4 and Figure S5). These results indicate that NYE1 protein conformation may be regulated by redox during leaf senescence. We had also tried to determine whether the Mg-dechelating activity of NYE1 is also regulated accordingly. Nevertheless, because only a trace enzymatic activity of NYE1 could be detected *in vitro* (Figure 3d and S3b), though much effort has been spent on optimizing the detection system, we could hardly conduct a precise analysis to quantify the effect of redox conditions on the enzymatic activity of NYE1. Being prepared with the wheat germ system, both NYE1-FLAG and mNYE1-FLAG predominantly expressed as reduced form of monomers (Figure 3c). With these observations, we reason that *in vivo*, NYE1 could have a much higher enzymatic activity in a physiological yet undefined environment, possibly functioning more efficiently as the oxidized dimers and/or oligomers formed in response to increasingly enhanced reaction oxygen species (ROS) content in senescing chloroplasts. A consistent observation is that in a time course analysis in the leaves of *N. benthamiana*, NYE1-FLAG existed mainly as reduced monomers at the initial stage of induced senescence (Figure 5d). In contrast, the reduced mNYE1-FLAG showed no activity in *in vitro* enzyme activity detection system (Figure 3c-d). This indicates that the CRM indeed affects the function of NYE1, likely through regulating its conformational change, which is possibly involved in metal ion binding/removal (Giles et al., 2003), or through participating in its posttranslational modifications, such as S-sulphydration (Aroca et al., 2015) and S-nitrosylation (Wang et al., 2006), or via yet unknown mechanisms.

In the time course analysis in the leaves of *N. benthamiana*, we found that NYE1-FLAG exhibited different conformations at different stages of induced senescence (Figure 5d), suggesting that the different conformations of NYE1 may function differentially. Magnesium (Mg) chelatase is a heterotrimeric complex that facilitates the insertion of Mg^{2+} into protoporphyrin IX during Chl biosynthesis (Rissler et al., 2002). This prompts us that the dimers and/or oligomers of NYE1 may be more efficient in removing magnesium than monomers. On the other hand, chloroplasts are the main target of ROS-linked damage during natural senescence as ROS detoxification capability declines with age (Khanna-Chopra, 2012), and chloroplast degeneration is accompanied by chlorophyll degradation and the progressive loss of proteins at the early stage of senescence (Lim et al., 2007). Of course, after being attacked by ROS, NYE1 also possibly forms insoluble aggregates, which are presumably destined to degradation. This is reminiscent of that in response to stresses, plants adopt NBR1-mediated selective autophagy to tackle insoluble ubiquitinated protein aggregates as an adaptive strategy (Zhou et al., 2013). Clearly, the significance of the CRM-mediated NYE1

conformational change awaits future investigation.

The CRM may have been evolved as a sensor of the changing redox potential to stimulate Chl degradation during leaf senescence, fruit ripening, and stress responses in higher plants

The CRM motif was exclusively present in NYE proteins among higher plants, neither in NYE/SGR-like (SGRL) proteins nor in the NYE/SGR proteins of the green algae *Chlamydomonas reinhardtii* and *Micromonas pusilla* (Matsuda et al., 2016, Hortensteiner, 2009). Although both NYE and SGRL possess Mg-dechelating activity *in vitro* (Matsuda et al., 2016, Shimoda et al., 2016), only NYE proteins seem to be involved in Chl degradation during leaf senescence *in vivo* (Sakuraba et al., 2014b). Curiously, it was recently reported that NYE/SGR of *C. reinhardtii* acts as Mg-dechelatease only during the formation of photosystem II rather than in Chl degradation (Chen et al., 2018). Here, we found that the CRM in NYE1 was indispensable for Chl degradation and Mg-dechelating activity during leaf senescence in *Arabidopsis* (Figure 2b, Figure 3d). These results imply that the CRM motif may have been evolved in higher plants to specifically mediate the Chl degradation function of NYEs/SGRs during leaf senescence. It has been known that an increase in the content of reactive oxygen species (ROS) is one of the earliest responses of plant cells upon senescence initiation (Khanna-Chopra, 2012). Our analysis shows that the CRM is critical for NYE1 to alter its conformational state in response to redox changes *in vivo* (Figure 5). Hence, we speculate that the CRM may be required for NYE1 to rapidly sense the changing redox potential to stimulate Chl degradation during leaf senescence. Whether the CRM is also necessary for NYE1/SGR1 to participate in other biological processes (Mur et al., 2010, Mecey et al., 2011, Zhou et al., 2011, Luo et al., 2013, Qian et al., 2016) requires further investigation. Like NYE1, PAO proteins also possess a C-terminal CRM, albeit structurally different (Gray et al., 2004); thus, it would be interesting to know that to what extent the redox regulation is also required for other CCEs to function properly.

MATERIALS AND METHODS

Plant Material and Growth Conditions

Arabidopsis thaliana wild-type (Col-0), *nye1* (*nye1-1*) (Ren et al., 2007), *nye1 nye2* (Wu et al., 2016), *pph-1* (Schelbert et al., 2009, Ren et al., 2010) and *N. benthamiana* were used in this study. The *nye1 nye2 pph* triple mutant was generated by genetically crossing *nye1 nye2* with *pph-1*. Plant transformation was conducted using a floral dip procedure (Clough and Bent, 1998). Putative transgenic plants were selected on MS medium supplemented with 100 mg/L kanamycin (for pCHF3-derived constructs). Both *Arabidopsis* and *N. benthamiana* were grown at 22–24°C, under long-day conditions (16 h light/8 h dark) in a growth chamber

equipped with cool-white fluorescent lights ($100 \mu\text{mol m}^{-2} \text{s}^{-1}$). For dark treatment, the 5-6th leaves detached from 3-week-old *Arabidopsis* plants were incubated on wet filter paper and kept in darkness at 22 °C for the indicated days.

Plasmid Construction

For both transient and stable expression assays, cDNAs of truncated mutants, point mutations and FLAG-tagged fusion proteins of NYE1 were amplified by specific primers and cloned into the pCHF3 vector (Ge et al., 2005). For complementation assays, a promoter fragment (1.5 kb) upstream of the *NYE1* start codon was pre-inserted into pCHF3 (pNYE1-pCHF3) and cDNAs of *NYE1*¹⁻²¹¹ and *NYE1*¹⁻²⁴² were amplified and cloned into the pNYE1-pCHF3 vector. Site-directed mutagenesis of residues in *NYE1* was performed by specific primers using a PCR-based quick change site-directed mutagenesis. For pull-down assays, the coding regions of *NYE1* and *mNYE1* without the predicted N terminal chloroplast transit peptide (48 aa) were amplified and separately cloned into pET28a (His-tag, Novagen) or pMAL-C5G (MBP-tag, NEB) vector. Full-length cDNAs of *CCGs* (*HCAR*, *NOL*, *PPH*, *PAO* and *RCCR*) and cDNA of NYC1¹⁻³⁴² were cloned into pMAL-C5G. For BiFC assays, full-length cDNAs of *NYE1* and *mNYE1* were cloned into the pXY103 (-nYFP) and pXY104 (-cYFP) vectors, and the cDNAs of *CCGs* (*NOL*, *PPH* and *RCCR*) were cloned into pXY104. For the yeast two-hybrid assay, cDNAs of truncated versions of *NYE1* were cloned into pGADT7, and *Lhcb1*, 2, 3 were cloned into pGBKT7.

Transient expression assays and BiFC assays

Transient expression and BiFC assays in the leaves of *N. benthamiana* were performed according to a previous study (Zhu et al., 2015).

High-Performance Liquid Chromatography (HPLC)

Chl and green Chl catabolites were extracted and analyzed using reverse-phase HPLC as described (Schelbert et al., 2009, Wu et al., 2016) with the following modifications. HPLC was performed on an Agilent 1260 Infinity LC System (Agilent) equipped with a Hanbon Phecda C18 column (250 mm × 4.6 mm, 5 μm) (Hanbon). The mobile phase consisted of solvent A [methanol : acetonitrile : 0.25M pyridine = 2:1:1 (v : v : v)] and solvent B [methanol : acetonitrile : acetone = 1:1:3 (v : v : v)], and an elution gradient from 80% B in A to 98% B in A within 6 min, followed by 98% B for 14 min. The flow rate was 1.2 mL/min. Chl catabolites were detected at 410 nm.

Mg-Dechelating Activity

Mg-dechelating activity of NYE1 was determined according to Shimoda et al. (2016).

Recombinant NYE1-FLAG, mNYE1-FLAG, NYE1^{Y82C}-FLAG, NYE1^{D88Y}-FLAG, NYE1^{I97M}-FLAG, NYE1^{W122R}-FLAG, and NYE1^{R151S}-FLAG proteins were prepared using the High-Yield Wheat Germ Protein Expression System (Promega). Chl *a* (Sigma) was used as substrate, and the Chl catabolites were analyzed by HPLC as described above.

Western Blot Analysis

Immunoblot analysis was performed according to Wu et al. (2016). Protein extracts were mixed with 1 volume of 2×sample buffer [100 mM Tris, 20% glycerol, 4% SDS (pH 6.8), and 0.04% bromophenol blue] in the presence (reducing) or absence (non-reducing) of 5 mM DTT or 5mM NEM. The mixed protein solutions were denatured at 95°C for 5 min, separated by SDS-PAGE on 10% polyacrylamide gels, and detected by immunoblots using anti-FLAG (Sigma), anti-MBP (TransGen) or anti-His antibodies (TransGen).

Pull-Down Assays

Pull-down assays were performed according to Zhu et al (2015). His-tagged and MBP-tagged fusion proteins were expressed in the *E. coli* strain BL21, and were extracted with extraction buffer [50 mM Tris-HCl (pH 7.5), 0.15 M NaCl, 0.2% Triton X-100, and protease inhibitor cocktail (Sigma)] with or without 0.1% SDS, respectively. For His-pull-down and MBP-pull-down, protein mixtures were incubated with 30 µl Ni-NTA metal affinity matrix (Sangon Biotech) and amylose resin (New England Biolabs), respectively. After incubation at 4 °C for 4 h, beads were washed eight times with column buffer [50 mM Tris-HCl (pH 7.5), 0.15 M NaCl, 0.2% Triton X-100]. Washed beads were boiled with 100 µl of 1×sample buffer [50 mM Tris, 10% glycerol, 2% SDS (pH 6.8), and 0.02% bromophenol blue] at 95°C for 5 min and subjected to immunoblot analysis using corresponding antibodies.

Yeast two-hybrid

Protein interactions between NYE1 truncated versions and LHCII subunits were analyzed according to the manufacturer's instruction manual (Clontech).

Accession numbers

NYE1 (AT4G22920), HCAR (AT1G04620), NYC1 (AT4G13250), NOL (AT5G04900), PPH (AT5G13800), PAO (AT3G44880), RCCR (AT4G37000), β-ACTIN2 (AT3G18780).

ACKNOWLEDGMENTS

We are grateful to Jianxiang Liu for sharing pXY103 and pXY104 vectors, and Tongshui Zhou and Guojun Zhou for technical assistance on HPLC analysis. This work was supported by grants from the National Natural Science Foundation of China (31670287) to BK, the

Science and Technology Commission of Shanghai Municipality (15JC1400800) to GR and the Swiss National Science Foundation (31003A_172977) to SH.

Reference

- ARMSTEAD, I., DONNISON, I., AUBRY, S., HARPER, J., HORTENSTEINER, S., JAMES, C., MANI, J., MOFFET, M., OUGHAM, H., ROBERTS, L., THOMAS, A., WEEDEN, N., THOMAS, H. & KING, I. 2006. From crop to model to crop: identifying the genetic basis of the staygreen mutation in the *Lolium/Festuca* forage and amenity grasses. *New Phytol*, 172, 592-597.
- ARMSTEAD, I., DONNISON, I., AUBRY, S., HARPER, J., HORTENSTEINER, S., JAMES, C., MANI, J., MOFFET, M., OUGHAM, H., ROBERTS, L., THOMAS, A., WEEDEN, N., THOMAS, H. & KING, I. 2007. Cross-species identification of Mendel's I locus. *Science*, 315, 73.
- AROCA, A., SERNA, A., GOTOR, C. & ROMERO, L. C. 2015. S-sulfhydration: a cysteine posttranslational modification in plant systems. *Plant Physiol*, 168, 334-342.
- AUBRY, S., MANI, J. & HORTENSTEINER, S. 2008. Stay-green protein, defective in Mendel's green cotyledon mutant, acts independent and upstream of pheophorbide a oxygenase in the chlorophyll catabolic pathway. *Plant Mol Biol*, 67, 243-256.
- BARRY, C. S., MCQUINN, R. P., CHUNG, M. Y., BESUDEN, A. & GIOVANNONI, J. J. 2008. Amino acid substitutions in homologs of the STAY-GREEN protein are responsible for the green-flesh and chlorophyll retainer mutations of tomato and pepper. *Plant Physiol*, 147, 179-187.
- BOROVSKY, Y. & PARAN, I. 2008. Chlorophyll breakdown during pepper fruit ripening in the chlorophyll retainer mutation is impaired at the homolog of the senescence-inducible stay-green gene. *Theor Appl Genet*, 117, 235-240.
- CHEN, J., ZHU, X., REN, J., QIU, K., LI, Z., XIE, Z., GAO, J., ZHOU, X. & KUAI, B. 2017. Suppressor of Overexpression of CO 1 Negatively Regulates Dark-Induced Leaf Degreening and Senescence by Directly Repressing Pheophytinase and Other Senescence-Associated Genes in Arabidopsis. *Plant Physiol*, 173, 1881-1891.
- CHEN, Y., SHIMODA, Y., YOKONO, M., ITO, H. & TANAKA, A. 2019. Mg-dechelate is involved in the formation of photosystem II but not in chlorophyll degradation in *Chlamydomonas reinhardtii*. *Plant J*, 97, 1022-1031.
- CHRIST, B., EGERT, A., SUSSENBACHER, I., KRAUTLER, B., BARTELS, D., PETERS, S. & HORTENSTEINER, S. 2014. Water deficit induces chlorophyll degradation via the 'PAO/phyllobilin' pathway in leaves of homoio- (*Cratogeomys pumilus*) and poikilochlorophyllous (*Xerophyta viscosa*) resurrection plants. *Plant Cell Environ*, 37, 2521-2531.

CHRIST, B., SCHELBERT, S., AUBRY, S., SUSSENBACHER, I., MULLER, T.,
KRAUTLER, B. & HORTENSTEINER, S. 2012. MES16, a member of the
methylesterase protein family, specifically demethylates fluorescent chlorophyll
catabolites during chlorophyll breakdown in Arabidopsis. *Plant Physiol*, 158,
628-641.

CHRIST, B., SUSSENBACHER, I., MOSER, S., BICHSEL, N., EGERT, A., MULLER, T.,
KRAUTLER, B. & HORTENSTEINER, S. 2013. Cytochrome P450 CYP89A9 is
involved in the formation of major chlorophyll catabolites during leaf senescence in
Arabidopsis. *Plant Cell*, 25, 1868-1680.

CLOUGH, S. J. & BENT, A. F. 1998. Floral dip: a simplified method for
Agrobacterium-mediated transformation of Arabidopsis thaliana. *Plant J*, 16,
735-743.

DELMAS, F., SANKARANARAYANAN, S., DEB, S., WIDDUP, E., BOURNONVILLE, C.,
BOLLIER, N., NORTHEY, J. G., MCCOURT, P. & SAMUEL, M. A. 2013. ABI3
controls embryo degreening through Mendel's I locus. *Proc Natl Acad Sci U S A*, 110,
E3888-E3894.

FANG, C., LI, C., LI, W., WANG, Z., ZHOU, Z., SHEN, Y., WU, M., WU, Y., LI, G., KONG,
L. A., LIU, C., JACKSON, S. A. & TIAN, Z. 2014. Concerted evolution of D1 and
D2 to regulate chlorophyll degradation in soybean. *Plant J*, 77, 700-712.

GAO, S., GAO, J., ZHU, X., SONG, Y., LI, Z., REN, G., ZHOU, X. & KUAI, B. 2016. ABF2,
ABF3, and ABF4 Promote ABA-Mediated Chlorophyll Degradation and Leaf
Senescence by Transcriptional Activation of Chlorophyll Catabolic Genes and
Senescence-Associated Genes in Arabidopsis. *Mol Plant*, 9, 1272-1285.

GE, X., DIETRICH, C., MATSUNO, M., LI, G., BERG, H. & XIA, Y. 2005. An Arabidopsis
aspartic protease functions as an anti-cell-death component in reproduction and
embryogenesis. *EMBO Rep*, 6, 282-288.

GILES, N. M., WATTS, A. B., GILES, G. I., FRY, F. H., LITTLECHILD, J. A. & JACOB, C.
2003. Metal and redox modulation of cysteine protein function. *Chem Biol*, 10,
677-693.

GRAY, J., CLOSE, P. S., BRIGGS, S. P. & JOHAL, G. S. 1997. A novel suppressor of cell
death in plants encoded by the Lls1 gene of maize. *Cell*, 89, 25-31.

HAUENSTEIN, M., CHRIST, B., DAS, A., AUBRY, S. & HORTENSTEINER, S. 2016. A
role for TIC55 as a hydroxylase of phyllobilins, the products of chlorophyll
breakdown during plant senescence. *Plant Cell*. 28,2510-2527.

HORTENSTEINER, S. 2009. Stay-green regulates chlorophyll and chlorophyll-binding
protein degradation during senescence. *Trends Plant Sci*, 14, 155-162.

JIANG, H., LI, M., LIANG, N., YAN, H., WEI, Y., XU, X., LIU, J., XU, Z., CHEN, F. & WU,

545 G. 2007. Molecular cloning and function analysis of the stay green gene in rice. *Plant*
546 *J*, 52, 197-209.

547 KHANNA-CHOPRA, R. 2012. Leaf senescence and abiotic stresses share reactive oxygen
548 species-mediated chloroplast degradation. *Protoplasma*, 249, 469-481.

549 KRAUTLER, B. 2014. Phyllobilins--the abundant bilin-type tetrapyrrolic catabolites of the
550 green plant pigment chlorophyll. *Chem Soc Rev*, 43, 6227-6238.

551 KUAI, B., CHEN, J. & HORTENSTEINER, S. 2018. The biochemistry and molecular
552 biology of chlorophyll breakdown. *J Exp Bot*, 69, 751-767.

553 LI, S., GAO, J., YAO, L., REN, G., ZHU, X., GAO, S., QIU, K., ZHOU, X. & KUAI, B. 2016.
554 The role of ANAC072 in the regulation of chlorophyll degradation during age- and
555 dark-induced leaf senescence. *Plant Cell Rep*, 35, 1729-1741.

556 LIM, P. O., KIM, H. J. & NAM, H. G. 2007. Leaf senescence. *Annu Rev Plant Biol*, 58,
557 115-136.

558 LUO, Z., ZHANG, J., LI, J., YANG, C., WANG, T., OUYANG, B., LI, H., GIOVANNONI, J.
559 & YE, Z. 2013. A STAY-GREEN protein SISGR1 regulates lycopene and
560 beta-carotene accumulation by interacting directly with SIPSY1 during ripening
561 processes in tomato. *New Phytol*, 198, 442-452.

562 MATSUDA, K., SHIMODA, Y., TANAKA, A. & ITO, H. 2016. Chlorophyll a is a favorable
563 substrate for Chlamydomonas Mg-dechelataase encoded by STAY-GREEN. *Plant*
564 *Physiol Biochem*, 109, 365-373.

565 MECEY, C., HAUCK, P., TRAPP, M., PUMPLIN, N., PLOVANICH, A., YAO, J. & HE, S. Y.
566 2011. A critical role of STAYGREEN/Mendel's I locus in controlling disease
567 symptom development during Pseudomonas syringae pv tomato infection of
568 Arabidopsis. *Plant Physiol*, 157, 1965-1974.

569 MEGURO, M., ITO, H., TAKABAYASHI, A., TANAKA, R. & TANAKA, A. 2011.
570 Identification of the 7-hydroxymethyl chlorophyll a reductase of the chlorophyll
571 cycle in Arabidopsis. *Plant Cell*, 23, 3442-3453.

572 MOU, Z., FAN, W. & DONG, X. 2003. Inducers of plant systemic acquired resistance
573 regulate NPR1 function through redox changes. *Cell*, 113, 935-944.

574 MUR, L. A., AUBRY, S., MONDHE, M., KINGSTON-SMITH, A., GALLAGHER, J.,
575 TIMMS-TARAVELLA, E., JAMES, C., PAPP, I., HORTENSTEINER, S., THOMAS,
576 H. & OUGHAM, H. 2010. Accumulation of chlorophyll catabolites photosensitizes
577 the hypersensitive response elicited by Pseudomonas syringae in Arabidopsis. *New*
578 *Phytol*, 188, 161-174.

579 PAN, J., TAN, J., WANG, Y., ZHENG, X., OWENS, K., LI, D., LI, Y. & WENG, Y. 2018.
580 STAYGREEN (CsSGR) is a candidate for the anthracnose (Colletotrichum orbiculare)
581 resistance locus cla in Gy14 cucumber. *Theor Appl Genet*, 131, 1577-1587.

582 PARK, S. Y., YU, J. W., PARK, J. S., LI, J., YOO, S. C., LEE, N. Y., LEE, S. K., JEONG, S.
583 W., SEO, H. S., KOH, H. J., JEON, J. S., PARK, Y. I. & PAEK, N. C. 2007. The
584 senescence-induced staygreen protein regulates chlorophyll degradation. *Plant Cell*,
585 19, 1649-1664.

586 PRUZINSKA, A., ANDERS, I., AUBRY, S., SCHENK, N., TAPERNOUX-LUTHI, E.,
587 MULLER, T., KRAUTLER, B. & HORTENSTEINER, S. 2007. In vivo participation
588 of red chlorophyll catabolite reductase in chlorophyll breakdown. *Plant Cell*, 19,
589 369-387.

590 PRUZINSKA, A., TANNER, G., ANDERS, I., ROCA, M. & HORTENSTEINER, S. 2003.
591 Chlorophyll breakdown: pheophorbide a oxygenase is a Rieske-type iron-sulfur
592 protein, encoded by the accelerated cell death 1 gene. *Proc Natl Acad Sci U S A*, 100,
593 15259-15264.

594 QIAN, L., VOSS-FELS, K., CUI, Y., JAN, H. U., SAMANS, B., OBERMEIER, C., QIAN, W.
595 & SNOWDON, R. J. 2016. Deletion of a Stay-Green Gene Associates with Adaptive
596 Selection in *Brassica napus*. *Mol Plant*, 9, 1559-1569.

597 QIU, K., LI, Z., YANG, Z., CHEN, J., WU, S., ZHU, X., GAO, S., GAO, J., REN, G., KUAI,
598 B. & ZHOU, X. 2015. EIN3 and ORE1 Accelerate Degreening during
599 Ethylene-Mediated Leaf Senescence by Directly Activating Chlorophyll Catabolic
600 Genes in *Arabidopsis*. *PLoS Genet*, 11, e1005399.

601 REN, G., AN, K., LIAO, Y., ZHOU, X., CAO, Y., ZHAO, H., GE, X. & KUAI, B. 2007.
602 Identification of a novel chloroplast protein AtNYE1 regulating chlorophyll
603 degradation during leaf senescence in *Arabidopsis*. *Plant Physiol*, 144, 1429-1441.

604 REN, G., ZHOU, Q., WU, S., ZHANG, Y., ZHANG, L., HUANG, J., SUN, Z. & KUAI, B.
605 2010. Reverse genetic identification of CRN1 and its distinctive role in chlorophyll
606 degradation in *Arabidopsis*. *J Integr Plant Biol*, 52, 496-504.

607 RISSLER, H. M., COLLAKOVA, E., DELLAPENNA, D., WHELAN, J. & POGSON, B. J.
608 2002. Chlorophyll biosynthesis. Expression of a second chl I gene of magnesium
609 chelatase in *Arabidopsis* supports only limited chlorophyll synthesis. *Plant Physiol*,
610 128, 770-779.

611 SAKURABA, Y., JEONG, J., KANG, M. Y., KIM, J., PAEK, N. C. & CHOI, G. 2014a.
612 Phytochrome-interacting transcription factors PIF4 and PIF5 induce leaf senescence
613 in *Arabidopsis*. *Nat Commun*, 5, 4636.

614 SAKURABA, Y., KIM, D., KIM, Y. S., HORTENSTEINER, S. & PAEK, N. C. 2014b.
615 *Arabidopsis* STAYGREEN-LIKE (SGRL) promotes abiotic stress-induced leaf
616 yellowing during vegetative growth. *FEBS Lett*, 588, 3830-3837.

617 SAKURABA, Y., PARK, S. Y., KIM, Y. S., WANG, S. H., YOO, S. C., HORTENSTEINER, S.
618 & PAEK, N. C. 2014c. *Arabidopsis* STAY-GREEN2 is a negative regulator of

chlorophyll degradation during leaf senescence. *Mol Plant*, 7, 1288-1302.

SAKURABA, Y., SCHELBERT, S., PARK, S. Y., HAN, S. H., LEE, B. D., ANDRES, C. B.,
KESSLER, F., HORTENSTEINER, S. & PAEK, N. C. 2012. STAY-GREEN and
chlorophyll catabolic enzymes interact at light-harvesting complex II for chlorophyll
detoxification during leaf senescence in Arabidopsis. *Plant Cell*, 24, 507-518.

SATO, Y., MORITA, R., KATSUMA, S., NISHIMURA, M., TANAKA, A. & KUSABA, M.
2009. Two short-chain dehydrogenase/reductases, NON-YELLOW COLORING 1
and NYC1-LIKE, are required for chlorophyll b and light-harvesting complex II
degradation during senescence in rice. *Plant J*, 57, 120-131.

SATO, Y., MORITA, R., NISHIMURA, M., YAMAGUCHI, H. & KUSABA, M. 2007.
Mendel's green cotyledon gene encodes a positive regulator of the
chlorophyll-degrading pathway. *Proc Natl Acad Sci U S A*, 104, 14169-14174.

SCHELBERT, S., AUBRY, S., BURLA, B., AGNE, B., KESSLER, F., KRUPINSKA, K. &
HORTENSTEINER, S. 2009. Pheophytin pheophorbide hydrolase (pheophytinase) is
involved in chlorophyll breakdown during leaf senescence in Arabidopsis. *Plant Cell*,
21, 767-785.

SHIMODA, Y., ITO, H. & TANAKA, A. 2016. Arabidopsis STAY-GREEN, Mendel's Green
Cotyledon Gene, Encodes Magnesium-Dechelataase. *Plant Cell*, 28, 2147-2160.

SONG, Y., YANG, C., GAO, S., ZHANG, W., LI, L. & KUAI, B. 2014. Age-triggered and
dark-induced leaf senescence require the bHLH transcription factors PIF3, 4, and 5.
Mol Plant, 7, 1776-1787.

WANG, Y., YUN, B. W., KWON, E., HONG, J. K., YOON, J. & LOAKE, G. J. 2006.
S-nitrosylation: an emerging redox-based post-translational modification in plants. *J*
Exp Bot, 57, 1777-1784.

WU, S., LI, Z., YANG, L., XIE, Z., CHEN, J., ZHANG, W., LIU, T., GAO, S., GAO, J., ZHU,
Y., XIN, J., REN, G. & KUAI, B. 2016. NON-YELLOWING2 (NYE2), a Close
Paralog of NYE1, Plays a Positive Role in Chlorophyll Degradation in Arabidopsis.
Mol Plant, 9, 624-627.

ZHOU, C., HAN, L., PISLARIU, C., NAKASHIMA, J., FU, C., JIANG, Q., QUAN, L.,
BLANCAFLOR, E. B., TANG, Y., BOUTON, J. H., UDVARDI, M., XIA, G. &
WANG, Z. Y. 2011. From model to crop: functional analysis of a STAY-GREEN gene
in the model legume *Medicago truncatula* and effective use of the gene for alfalfa
improvement. *Plant Physiol*, 157, 1483-1496.

ZHOU, J., WANG, J., CHENG, Y., CHI, Y. J., FAN, B., YU, J. Q. & CHEN, Z. 2013.
NBR1-mediated selective autophagy targets insoluble ubiquitinated protein
aggregates in plant stress responses. *PLoS Genet*, 10, e1004477.

ZHU, X., CHEN, J., QIU, K. & KUAI, B. 2017. Phytohormone and Light Regulation of

656 Chlorophyll Degradation. *Front Plant Sci*, 8, 1911.
657 ZHU, X., CHEN, J., XIE, Z., GAO, J., REN, G., GAO, S., ZHOU, X. & KUAI, B. 2015.
658 Jasmonic acid promotes degreening via MYC2/3/4- and ANAC019/055/072-mediated
659 regulation of major chlorophyll catabolic genes. *Plant J*, 84, 597-610.
660

Legends

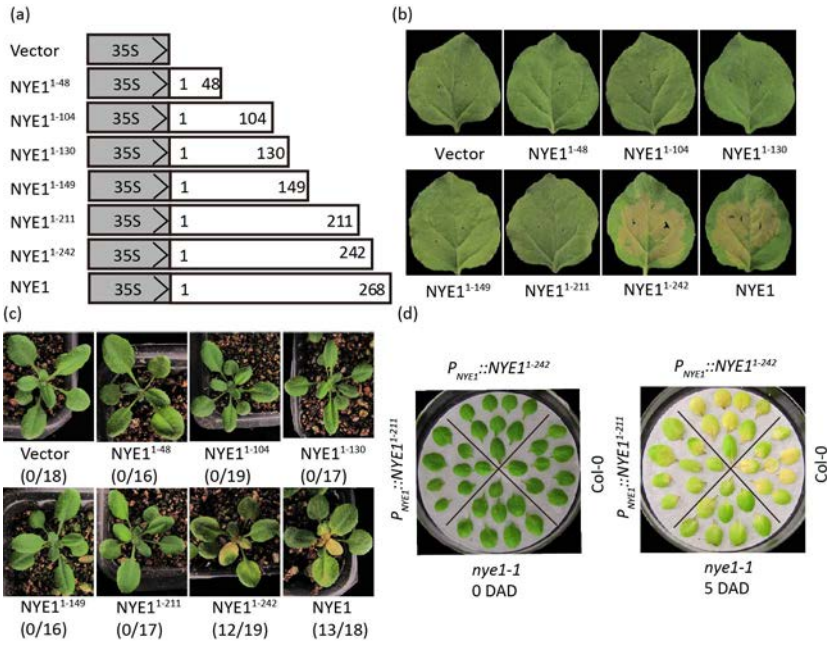


Figure 1. Identification of the functional domains of NYE1 proteins.

(a) Schematic of the NYE1 cDNA truncations used in this work. NYE1 expression was driven by the 35S promoter. Phenotypes of 4-week-old *N. benthamiana* leaves at 2 d post infiltration (dpi) with Agrobacteria carrying constructs for the expression of full length NYE1, respective truncated versions, or an empty vector.

(c) Phenotypes of 3-week-old T1 transgenic *nyel-1* plants expressing full length NYE1, respective truncated versions, or an empty vector. The numbers in brackets indicate the ratios of plants with albino or yellowish leaves to total plants.

(d) Genetic complementation of *nyel-1* with NYE1¹⁻²¹¹ and NYE1¹⁻²⁴², respectively. Phenotypes of the excised 5-6th leaves of Col-0, *nyel-1*, *P_{NYE1}::NYE1¹⁻²¹¹*, and *P_{NYE1}::NYE1¹⁻²⁴²* plants before (0 DAD) and after dark treatment for 5 d (5 DAD).

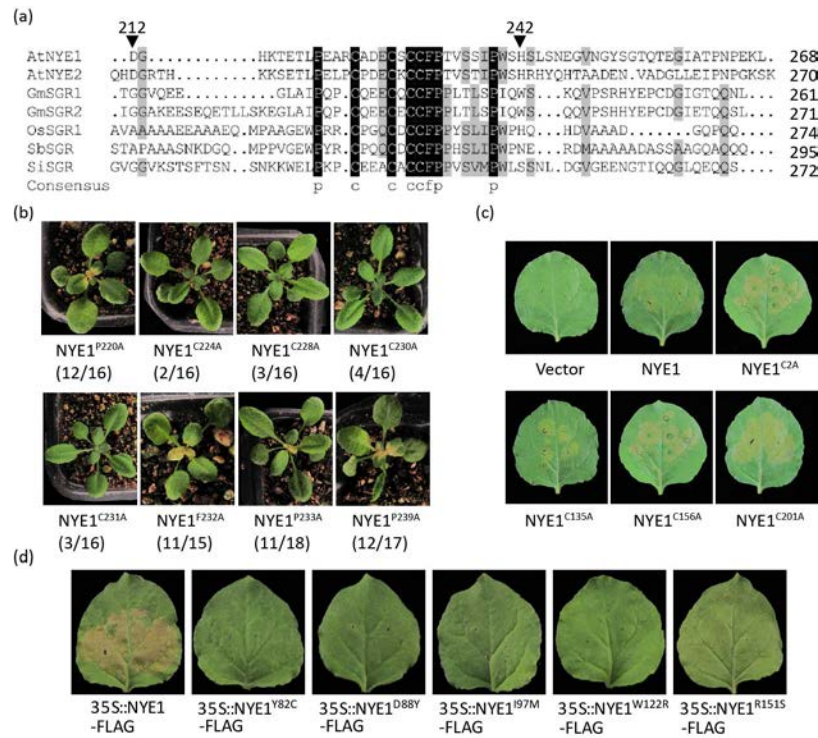


Figure 2. Functional characterization of eight conserved residues within the CRM, four cysteines scattering upstream of CRM and five reported key residues in the core domain of NYE1.

(a) Alignment of the cysteine-rich motifs of NYE1 sequences from different higher plant species. Sequences were aligned by DNAMAN software. Black shading and dark gray shading represent 100% and 75% sequence identities, respectively. GenBank protein accession numbers are as follows: *Arabidopsis thaliana* AtNYE1, AAW82962; AtNYE2, AAU05981; *Glycine max* GmSGR1, AAW82959; GmSGR2, AAW82960; *Oryza sativa* OsSGR1, AAW82954; *Sorghum bicolor* SbSGR, AAW82958; *Solanum lycopersicon* SISGR, ACB56587.

(b) Phenotypes of 3-week-old T1 transgenic *nye1-1* plants expressing NYE1 with single point mutations in the cysteine-rich motif. The numbers in brackets indicate the ratios of plants with albino or yellowish leaves to total plants.

(c) Phenotypes of *N. benthamiana* leaves at 2 dpi with Agrobacteria carrying constructs for the expression of NYE1, NYE1^{C2A}, NYE1^{C135A}, NYE1^{C156A}, and NYE1^{C201A}, or an empty vector.

(d) Phenotypes of *N. benthamiana* leaves at 1.5 dpi with Agrobacteria containing constructs for the expression of NYE1-FLAG, NYE1^{Y82C}-FLAG, NYE1^{D88Y}-FLAG, NYE1^{I97M}-FLAG, NYE1^{W122R}-FLAG, and NYE1^{R151S}-FLAG.

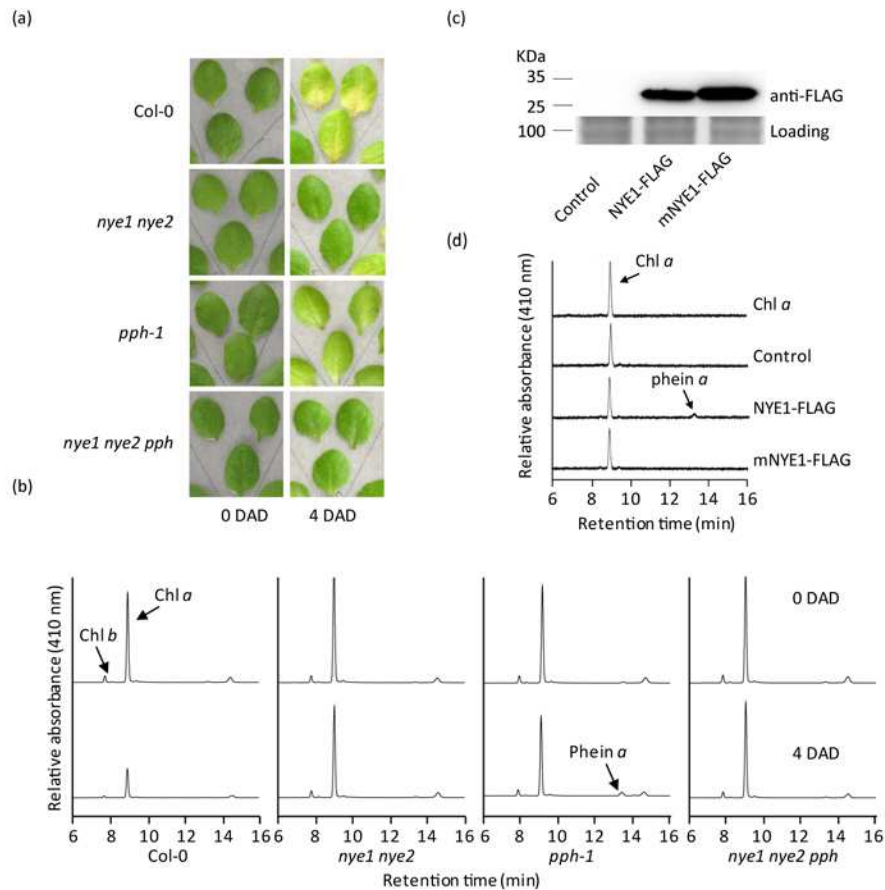


Figure 3. The CRM is necessary for the Mg-dechelating activity of NYE1.

(a) Phenotypes of the indicated genotypes after dark treatment. Rosette leaves detached from 4-week-old plants were treated in darkness for 4 d. DAD, days after dark treatment.

(b) HPLC examination of the leaves shown in (a). Chl, chlorophyll; phe, pheophytin; DAD, days after dark treatment.

(c) Immunoblot analysis of NYE1-FLAG and mNYE1-FLAG proteins expressed with the wheat germ protein expression system under non-reducing condition using a monoclonal anti-FLAG-HRP antibody.

(d) HPLC examination after incubating chlorophyll *a* with NYE1-FLAG and mNYE1-FLAG prepared with the wheat germ protein expression system. The chloroplast transit peptides of NYE1 and mNYE1 were removed, and the FLAG-tag fused to their C-termini. Chl, chlorophyll; phe, pheophytin.

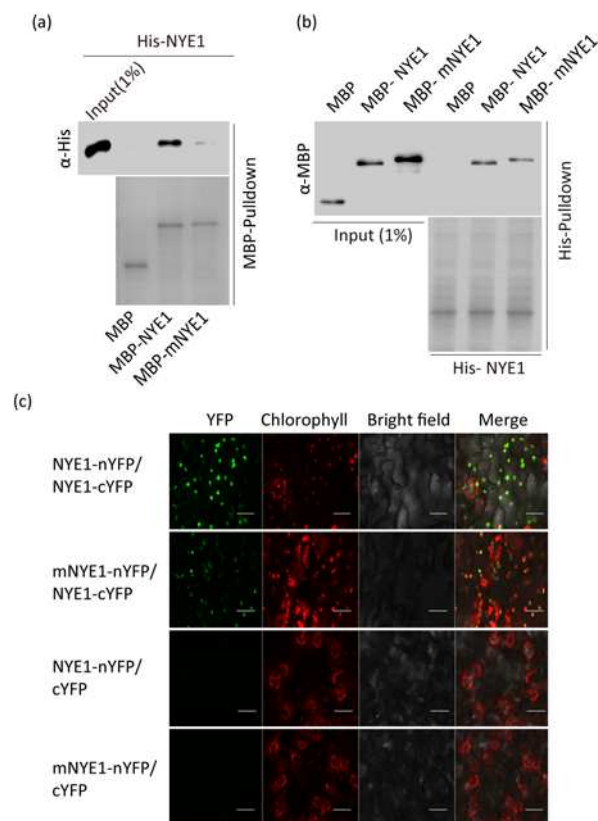


Figure 4. Requirement of the cysteines in the CRM for NYE1 self-interaction.

- (a) Interaction analysis of MBP-NYE1, MBP-mNYE1, and free MBP with His-NYE1 in an MBP-pull-down assay.
- (b) Interaction analysis of His-NYE1 with MBP-NYE1, MBP-mNYE1, and free MBP in a His-pull-down assay.
- (c) BiFC analysis in *N. benthamiana* leaves of combinations of NYE1-nYFP or mNYE1-nYFP with NYE1-cYFP or free cYFP. YFP, YFP fluorescence; Chlorophyll, chlorophyll autofluorescence; Bright field, white light; Merge, overlay of all three images. Scale bar=20 μ m.

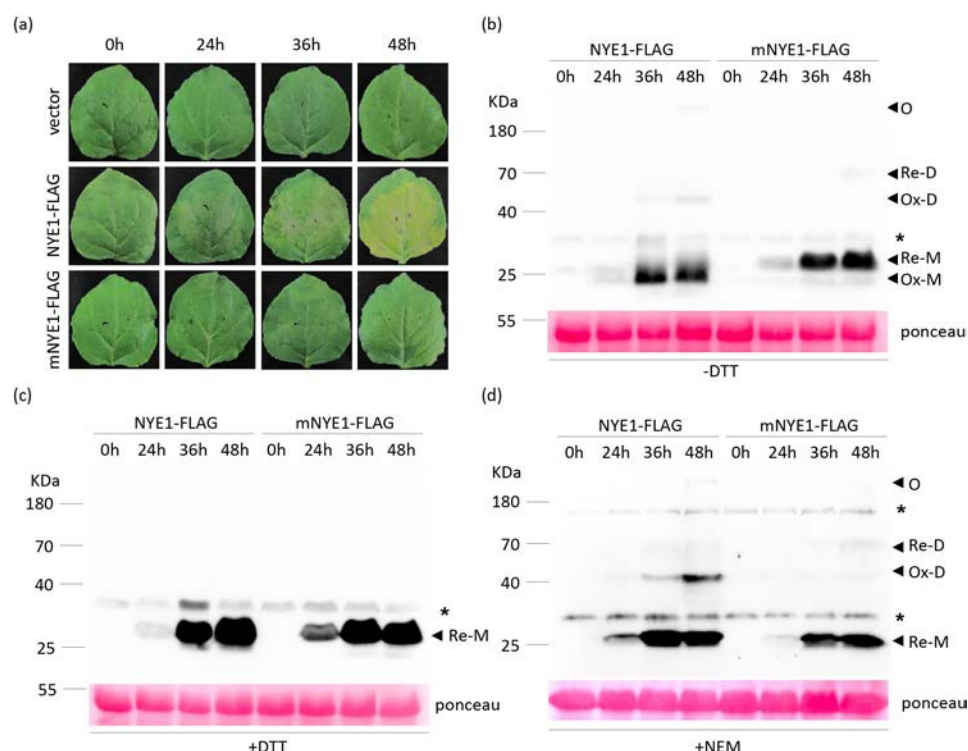


Figure 5. Western blot analysis of *in vitro* and *in vivo* NYE1 and mNYE1 protein conformations.

(a) Phenotypes of the leaves of 4-week-old *N. benthamiana* at 24 h, 36 h and 48 h post infiltration with Agrobacteria containing constructs for the 35S promoter-driven expression of NYE1-FLAG or mNYE1-FLAG, or an empty vector.

(b), (c) and (d) Immunoblot analysis under non-reducing [without DTT; (b)] or reducing conditions [5 mM DTT; (c)] or 5 mM NEM (d) of NYE1-FLAG and mNYE1-FLAG before (0 h) or 24 h, 36 h, and 48 h after infiltration using a monoclonal anti-FLAG-HRP antibody. “*”, non-specific proteins; “O”, oligomers; “Re-D”, reduced dimers; “Ox-D”, oxidized dimers; “Re-M”, reduced monomers; “Ox-M”, oxidized monomers.

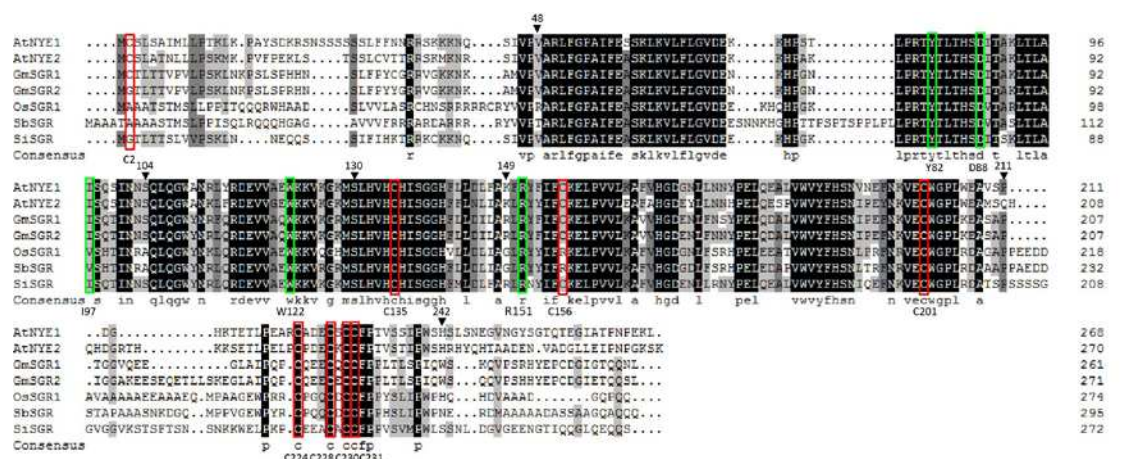


Figure S1. Alignment of NYE protein sequences from higher plants.

Sequences were aligned by DNAMAN software. Black shading, dark gray shading, and gray shading represent 100%, 75%, and 40% sequence identities, respectively. GenBank protein accession numbers are as follows: *Arabidopsis thaliana* AtNYE1, AAW82962; AtNYE2, AAU05981; *Glycine max* GmSGR1, AAW82959; GmSGR2, AAW82960; *Oryza sativa* OsSGR1, AAW82954; *Sorghum bicolor* SbSGR, AAW82958; *Solanum*

lycopersicon SISGR, ACB56587. Red rectangles highlight the positions of eight cysteine residues; Green rectangles highlight the positions of five reported key residues in the core domain of NYE1.

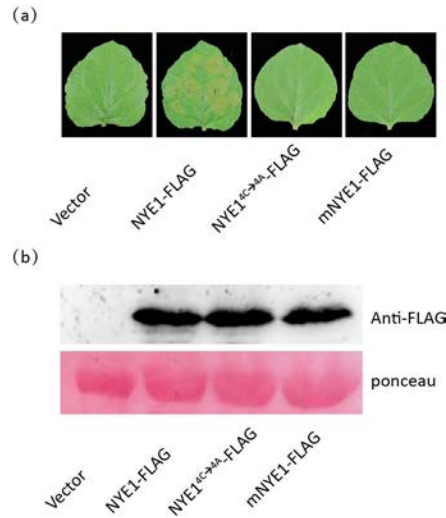


Figure S2. Functional characterization of NYE1^{4C→4A}-FLAG and mNYE1-FLAG in *N. benthamiana* leaves.

(a) Phenotypes of 4-week-old *N. benthamiana* leaves at 2 dpi with Agrobacteria carrying respective constructs.

mNYE1-FLAG, NYE1^{C224G/C228G/C230G/C231G}-FLAG; NYE1^{4C→4A}-FLAG, NYE1^{C224A/C228A/C230A/C231A}-FLAG.

(b) Immunoblot analysis of *N. benthamiana* leaves infiltrated with respective constructs shown in (a). 5 mM DTT was added during sample preparation.

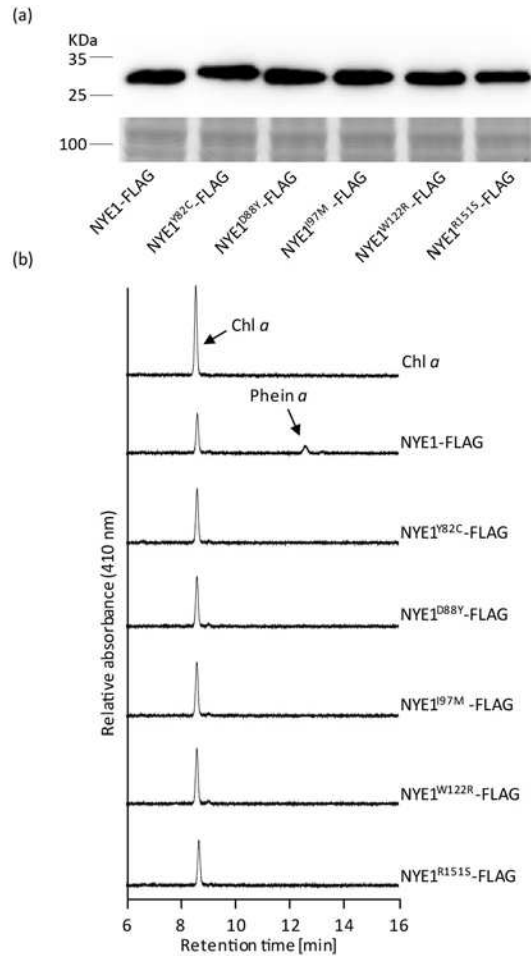


Figure S3. The Y82, D88, I97, W122, and R151 residues are required for the Mg-dechelating activity of NYE1

(a) Immunoblot analysis of NYE1-FLAG, NYE1^{Y82C}-FLAG, NYE1^{D88Y}-FLAG, NYE1^{I97M}-FLAG, NYE1^{W122R}-FLAG, and NYE1^{R151S}-FLAG proteins prepared by the wheat germ protein expression system under non-reducing condition using a monoclonal anti-FLAG-HRP antibody.

(b) HPLC examination of Chl catabolites. Chl *a* was incubated with crude extracts of either wild-type or respective mutated NYE1 proteins shown in (a) in the Mg-dechelating reaction buffer for 60 minutes. Chl, chlorophyll; phe, pheophytin.

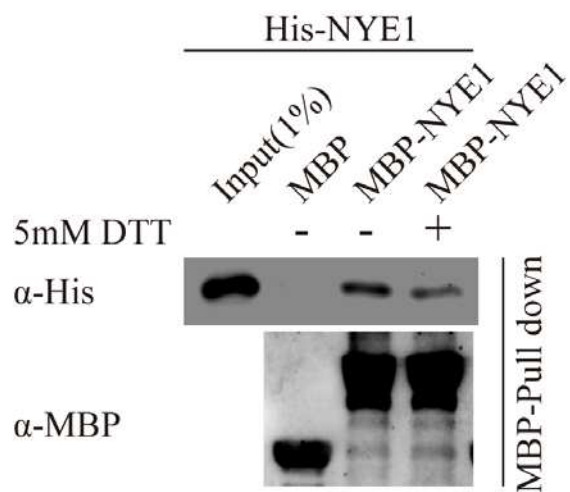


Figure S4. MBP pulldown assay examined the NYE1 self-interaction ability under both non-reducing (-5mM DTT) and reducing condition (+5mM DTT). Pulled-down proteins were detected by immunoblotting using both monoclonal anti-His and anti-FLAG antibodies.

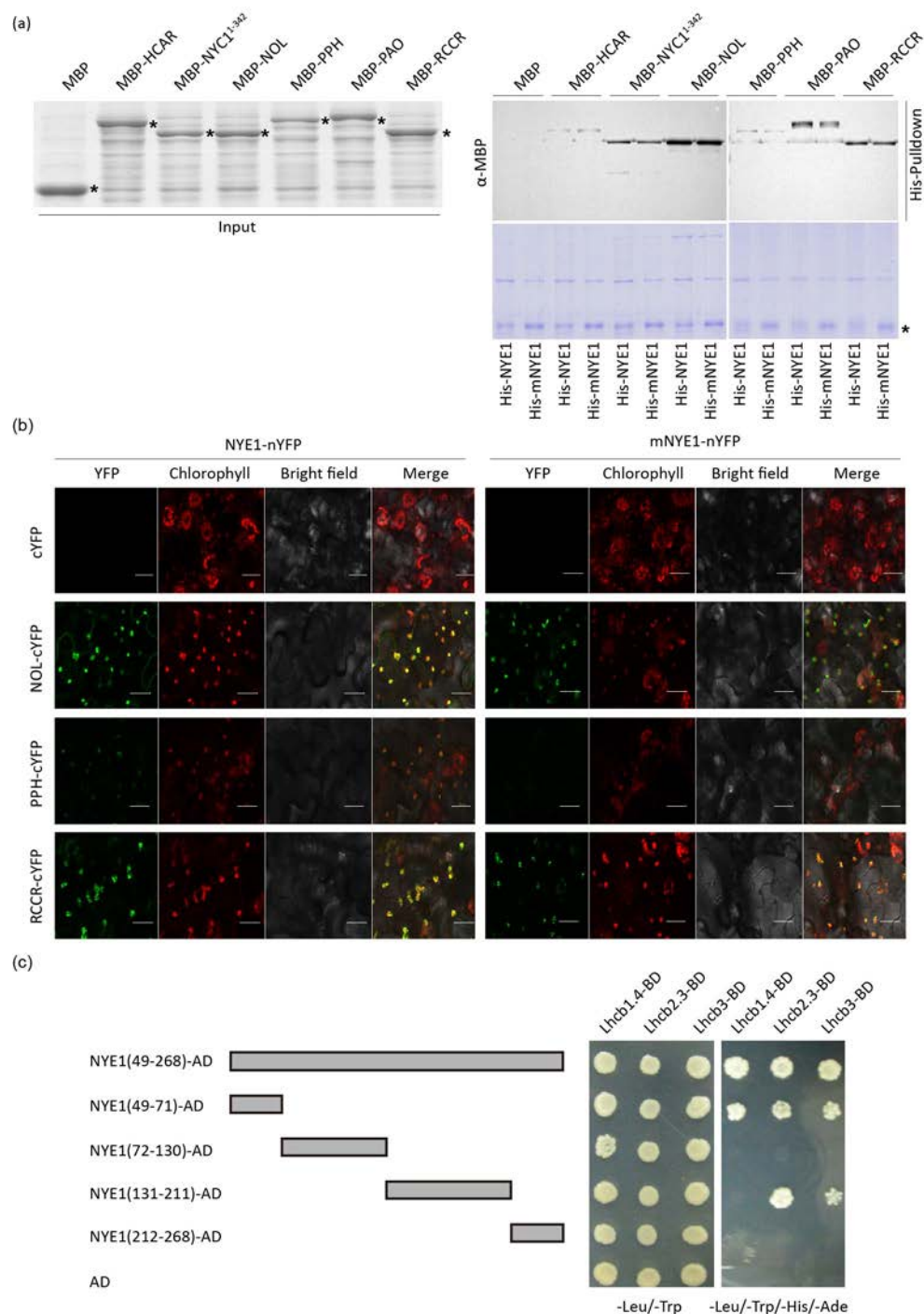


Figure S5. Similar interaction capabilities between NYE1 and mNYE1 with CCEs and LHCII subunits *in vitro* and *in vivo*.

(a) Interaction capabilities of MBP-CCEs with His-NYE1 or His-mNYE1 in pull-down assays. Pulled-down proteins were detected by immunoblotting using a monoclonal anti-His antibody. “*” indicates corresponding MBP-CCEs proteins, His-NYE1 or His-mNYE1.

(b) BiFC interaction assays of NYE1-nYFP or mNYE1-nYFP with CCE-cYFPs in *N. benthamiana* leaves. YFP, YFP fluorescence; Chlorophyll, chlorophyll autofluorescence; Bright field, white light; Merge, overlay of all three images. Scale bar=20 um.

(c) Yeast-two-hybrid analysis of interactions between different truncated NYE1 fragments and three Lhcb

752 proteins. All the three Lhcb subunits were